Synthesis of Reconfigurable Multiple Shaped Beams of a Concentric Circular Ring Array Antenna Using Evolutionary Algorithms

Sanjay Kumar Dubey[1] and Debasis Mandal[2]

[1]*K. K. University, Bihar, India,*
[2]*Department of Electronics and Communication Engineering, Ramchandra Chandravansi University, Bishrampur, Palamu, Jharkhand, India*

https://doi.org/10.26636/jtit.2023.168022

Abstract — The approach described in this paper uses evolutionary algorithms to create multiple-beam patterns for a concentric circular ring array (CCRA) of isotropic antennas using a common set of array excitation amplitudes. The flat top, cosec^2, and pencil beam patterns are examples of multiple-beam patterns. All of these designs have an upward angle of $\theta = 0°$. All the patterns are further created in three azimuth planes ($\varphi = 0°$, 5°, and 10°). To create the necessary patterns, non-uniform excitations are used in combination with evenly spaced isotropic components. For the flat top and cosecant-squared patterns, the best combination of common components, amplitude and various phases is applied, whereas the pencil beam pattern is produced using the common amplitude only. Differential evolutionary algorithm (DE), genetic algorithm (GA), and firefly algorithm (FA) are used to generate the best 4-bit discrete magnitudes and 5-bit discrete phases. These discrete excitations aid in lowering the feed network design complexity and the dynamic range ratio (DRR). A variety of randomly selected azimuth planes are used to verify the excitations as well. With small modifications in the desired parameters, the patterns are formed using the same excitation. The results proved both the efficacy of the suggested strategy and the dominance of DE over GA as well as FA.

Keywords — cosec^2 beam, differential evolution algorithm (DE), firefly algorithm (FA), flat top beam, genetic algorithm (GA), multiple shaped beam patterns, pencil beam

1. Introduction

The concentric ring array antenna with 360°azimuthal symmetry is highly helpful in wireless communications, especially for satellite and radar-related applications. Furthermore, a large sidelobe with a significant ripple issue was observed while producing the structured beams, including the flat-top, cosec^2, as well as pencil-shaped beam, at a variety of azimuth planes with similar excitation amplitudes. A variety of methods exist for creating array patterns and multiple beam patterns that have been documented in literature. These include, inter alia, [1]–[14]. With the help of a simulated annealing optimization technique, Diaz *et al*. suggested, in paper [5], a technique which enables the effective synthesis of multiple-patterns of linear array antennas characterized by constant amplitude dispersals that differ in phase only. An efficient iterative approach for the power synthesis of programmable array antennas is provided by Buttazzoni and Vescovo in [6]. The approach is applicable to arrays of any shape, covering situations when there are many items present. The excitation magnitude of every array element remains unchanged throughout the configuration process thanks to phase-only control, which determines how reconfigurability is accomplished.

According to a procedure suggested and created by Lei *et al*. in [7], an isotropic array of linear antenna components may produce a cosecant-squared beam pattern by including optimal amplitudes and phases. Paper [8] shows that a single array antenna may need to emit more than one pattern per area or financial constraints. Each pattern is chosen and electronically controlled in way, where only the phase may be changed. With such a scenario, a synthesis approach is provided that can simultaneously calculate the common amplitude and the individual phases. Additionally, the strategy is adaptable enough to accommodate extra restrictions and permits an effective deployment. Phase-only as well as amplitude-phase syntheses of an identical dual beam pattern of a linear array antenna employing real-valued and floating-point genetic algorithms are compared by Mahanti *et al*. in paper [9], with sum and sector array patterns serving as two examples.

To create customized beam patterns, uniform as well as Gaussian distributions of identical magnitude are used (flat top and cosec^2). Additionally, various beam patterns require distinct kinds of phases. Durr *et al*. in [10] proposed the Woodward-Lawson approach to identify such excitations. With the use of evolution algorithms, Dubey and Mandal [11] describe a pattern synthesis technique for creating dual array patterns of an isotropic planar array antenna of rectangular shape. The cosec^2 pattern and a pencil beam pattern are two examples of dual-beam patterns that are both directed at an upper angle of twenty degrees. Chakraborty *et al*. in [12] pro-

vide a technique for figuring out the phase allocation of an array having a linear structure of discrete excitations with a given array pattern with specified aperture magnitude distributions. The infinite series, whose terms are individually expressed as integrals, is created from the specific series that represents the beam pattern. The asymptotic assessment of the integral using the stationary phase approach serves as the basis for synthesis. Sector and cosecant beam computed outcomes are displayed. Again, for shaped-beam radiation patterns and a synthesis utilizing both line sources or evenly separated arrays, Stutzman [13] introduces the iterative sampling technique. A number of corrective patterns are applied to an original pattern that approximates the intended pattern. This method is used repeatedly until the required performance is attained. A matching set of adjustments leads to the discovery of the current distribution. Numerous examples demonstrate the possibility of obtaining patterns having either low major-beam ripple (Δ), low sidelobe level, or abrupt separation from the main lobe.

Using the concentric ring array antenna's best combinations of radial magnitudes and phases, Chatterjee *et al*. [14], [15] suggested a technique for producing twin beams. The gravitational search algorithm (GSA) is used to generate such excitations. They also suggested using the firefly algorithm (FA) to create the dual configuration for an array of concentric rings of antennas. The excitations employed in the circles of the CCAA uphold the supplied components, which are isotropic. By applying particular modes or switching combinations, the intended patterns are produced. Mangoud and Elragal [16] suggested using the enhanced practical swarm optimization (EPSO) method to create patterns from linear arrays. To increase the precision of the converging of traditional PSO, updated formulae of the global optimal particle location and velocities are adjusted. To produce adaptable wide nulls steered under the limitations of peak SLL as well as lowest principal beam width, the cumulative several deep nulls technique and the straight weights perturbations technique are taken into consideration. By carefully adjusting an element's existing magnitude or complex weights, beginning with the original Chebyshev pattern, one or more broad nulls may be produced, which can then be either symmetrically or asymmetrically oriented with respect to the primary beam.

Using a rectangular array of isotropic antennas, Mandal *et al*. offer, in [17], a pattern synthesis technique focused on the differential evolution algorithm (DE) to generate twin beam patterns. These include the pencil beam pattern plus the cosec^2 pattern. Such patterns are created by determining the best possible combinations of identical element magnitudes and phases for the cosec^2 pattern alone. To simplify the construction of the feed network, 5-bit discrete phases with 4-bit discrete amplitudes are employed. In article [18], the methods for keeping lower minor lobes in concentric ring array (CRA) antennas are thoroughly reviewed. The level of peak SLL reduction across a predetermined round field-of-view is suggested for directional uniform-amplitude concentric circular ring array antennas, thus introducing an iterative convex optimization (ICO)-driven array design synthesis methods. The ICO method optimizes the circle radii with the rotational angle for a particular size of rings and the size of equally balanced items within each ring, with potential limits on the minimum component spacing and greatest array size. Yi Jiang *et al*. [19] introduced modified integer genetic algorithm that gets around the ineffective searching and the significant processing burden of genetic algorithms. IIGA is used in [19] to create uniformly stimulated concentric ring arrays having aperture diameters ranging from tiny to larger, where the diameter of the array is nearly 50λ. All of the arrays that were produced adhere to the half-wavelength optimum component separation requirement.

In this paper, flat top, cosec^2, and pencil beam patterns of an antenna with sixty isotropic components are obtained by applying evolutionary algorithms to identify the best combination of common element magnitudes for all patterns as well as a band of phases for the flat top and cosec^2 shaped beam. Here, the geometry of the array is a concentric circle. The excitations produced through DE, FA, and GA were used to construct the patterns in three predetermined azimuth planes. With this method, instead of using a singular φ plane, it is additionally confirmed that the patterns maintain their required characteristics across a variety of azimuth planes. These have also been demonstrated by choosing a random set of φ planes, applying the identical excitations with each evolutionary algorithm, and obtaining patterns that are comparable but with a few slight differences. For a reduced dynamic range ratio (DRR), the acquired magnitude (4-bit) and phases (5-bit) are indeed digitized. Such discontinuous excitations are employed to reduce the feed network's design complexity, since they produce fewer attenuators as well as phase shifters due to the reduced DRR. These three evolutionary algorithms: differential evolution algorithms (DE), firefly algorithms (FA), and genetic algorithms are compared in terms of performance.

2. Problem Formulation

An array with a concentric circular layout, consisting consists of isotropic components is depicted in Fig. 1. The array pattern in the far field may be put into the following terms [1]–[3]:

$$AF(\theta,\varphi)=\sum_{m=1}^{M}\sum_{n=1}^{N} I_{mn}\mathrm{e}^{\mathrm{j}[kr_m\sin\theta\cos(\varphi-\varphi_{mn})+\alpha_{mn}}, \quad (1)$$

where:

- m = quantity of concentric circles,
- in the m-th ring, the number of isotropic components is N_m,
- I_{mn} = excitation magnitudes of mn-th component,
- d_m = inter-component rotational gaping (0.5λ),
- θ, φ = vertical and horizontal angle, item $\varphi_{mn}=\frac{2n\pi}{N_m}$ the arc stand of mn-th component; the range on n mentioned as $1\leqslant n\leqslant N_m$,
- $r_m=\frac{N_m d_m}{2\pi}$ radial distance of m-th ring,
- the wave number is denoted as $k=\frac{2\pi}{\lambda}$.

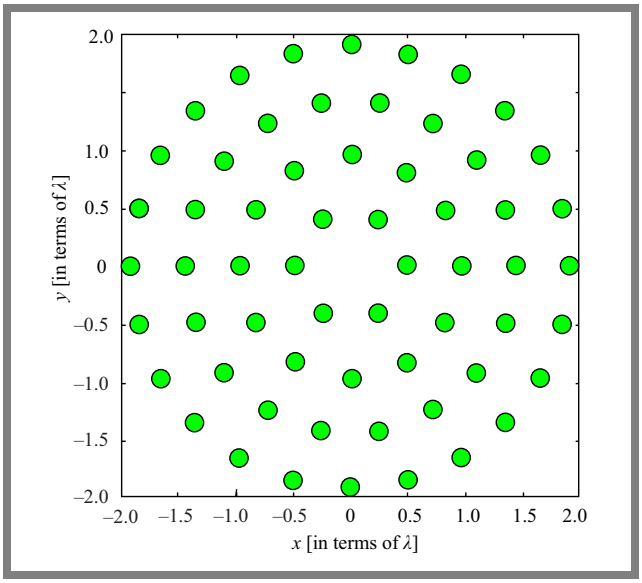

Fig. 1. Geometry of a CCRA array of 60 isotropic elements.

The objective functions of multiple shaped beam patterns are expressed as:

$$F(\rho) = k_1 \left\{ peakSLL^{d_1} - \max_{\theta \in A_1} \left[AF^{\rho}_{dB}(\theta, \varphi) \right] \right\}^2 + k_2 \times \Delta_1 + k_3 \left\{ peakSLL^{d_2} - \max_{\theta \in A_2} \left[AF^{\rho}_{dB}(\theta, \varphi) \right] \right\}^2 + k_4 \times \Delta_2 + k_5 \left\{ peakSLL^{d_3} - \max_{\theta \in A_3} \left[AF^{\rho}_{dB}(\theta, \varphi) \right] \right\}^2 , \tag{2}$$

where Δ_1 and Δ_2 are defined as:

$$\Delta_1 = \sum_{\theta_{ripple} \in \{0 \text{ to } 30^\circ\}} \left| AF^{\rho}_{dB}(\theta_{ripple}, \varphi) - D_{1dB}(\theta_{ripple}, \varphi) \right| , \tag{3}$$

$$\Delta_2 = \sum_{\theta_{ripple} \in \{-15 \text{ to } +15^\circ\}} \left| AF^{\rho}_{dB}(\theta_{ripple}, \varphi) - D_{2dB}(\theta_{ripple}, \varphi) \right| . \tag{4}$$

In Eq. (2), ρ is the unspecified parameter combination for both techniques and is expressed as:

$$\rho = I_{mn}, \alpha 1_{mn}, \alpha 2_{mn}; \quad \begin{cases} 1 \leqslant m \leqslant M, \\ 1 \leqslant n \leqslant N_m, \end{cases} \tag{5}$$

$peakSLL^{d_1}$, $peakSLL^{d_2}$ and $peakSLL^{d_3}$ are the expected outcomes of max SLL, while A_1, A_2 and A_3 are the sidelobe regions for the cosec^2 beam, flat top beam and pencil beam pattern, respectively. $D_{1dB}(\theta_{ripple}, \varphi)$ and $D_{2dB}(\theta_{ripple}, \varphi)$ are the desired patterns at azimuthal angles of $0^\circ, 5^\circ$ and 10° planes for cosec^2 beam and flat top array pattern, respectively. The estimated span of θ_{ripple} for the cosec^2 pattern ranges from 0° to 30° and for the flat top array pattern from -15 to 15 degrees. k_1, k_2, k_3, k_4, and k_5 are the weighting factors. With the use of several evolutionary algorithms, such as the DE, GA, and FA, these objective functions must be reduced to their minimum value.

3. Evolution Algorithm (EA)

3.1. Overview of Differential Evolution Algorithm

Evolutionary algorithms have been widely applied in a variety of problem areas over the past decade, and they have consistently found near-optimal solutions. DE is one such evolutionary method, and a full description and its features may be found in [20]–[26]. DE offers the following benefits: a straightforward construction, simplicity of use, efficiency, and durability for using in real-world situations. It has been used to find effective solutions to virtually intractable issues in a variety of scientific and engineering applications, without relying on expert knowledge or sophisticated design procedures. DE can provide the mechanism for obtaining the highest potential performance from a system that may be properly assessed. It uses mutations as a search query, with directing its searches towards the most probable locations in the available space. Using selection processes, genetic algorithms build a succession of populations. Crossover and mutation have been applied as search techniques in GAs.

The major difference between GAs and DE would be that GAs rely on the crossover approach to discover effective options, i.e. a stochastic and beneficial process for exchanging information across alternatives. So, even though evolutionary processes utilize mutation also as their primary search framework, DE seems to be an inhabitant searching technique which is capable of populating D-dimensional factor matrices with NP elements for each repetition. If there is no data about the situation, the starting crowd is chosen randomly. In a situation with an accessible preparatory answer, the initialization is often increased by combining uniformly distributed random variances to the existing preliminary solution. DE is based on such a revolutionary and experimental factor generation mechanism.

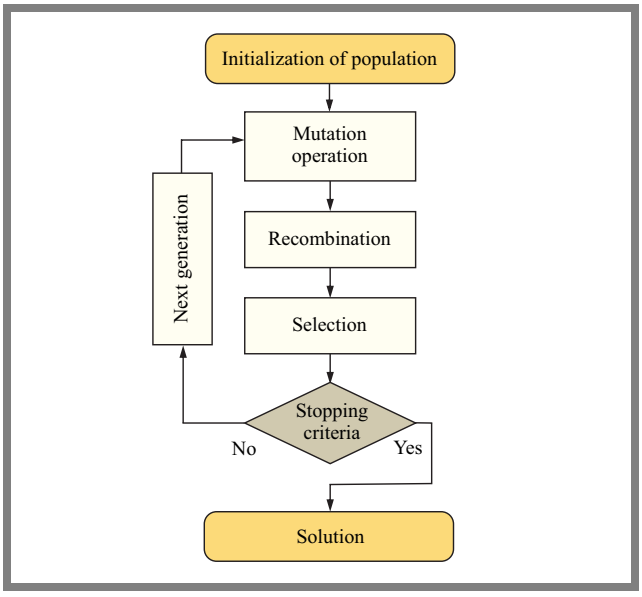

Fig. 2. Differential evolution algorithm (DE) flow chart.

Figure 2 depicts the DE process. The aim is to reduce function $f(Y)$, such as:

$$Y = [y_1,\, y_2,\, y_3,\, y_4, \ldots,\, y_{D_1}]\,, \tag{6}$$

where D_1 is the dimensionality or quantity of the search area. The population matrix as well as the assumed size N_1 of population are presented as follows:

$$y^g_{n,i} = [y^g_{n,1},\, y^g_{n,2},\, y^g_{n,3},\, y^g_{n,4}, \ldots,\, y^g_{n,D_1}]\,, \tag{7}$$

where $n = 1,\, 2,\, 3, \ldots, N_1$, and g is the number of iterations. The starting population is produced randomly between the higher y^H and lower bounds of y^L. The DE algorithm has three main steps: mutation, recombination, and selection which follow randomized initialization as well as creation in D_1 dimensionality searching field.

Three distinct vectors, y^g_{r1n}, $y^g_{r2n}$and y^g_{r3n}, were chosen from each input vector for the mutation procedure. Now it is possible to write the donor vectors s^{g+1}_n as:

$$s^{g+1}_n = y^g_{r1n} + F(y^g_{r2n} - y^g_{r3n})\,, \tag{8}$$

where scale factor F has a value ranging from 0 to 1.

Target vector $y^g_{n,i}$ and donor vector $s^{g+1}_{n,i}$ are used to create the trial vector $t^{g+1}_{n,i}$ during the recombination procedure. The target function values are finally weighed against each target vector $y^g_{n,i}$ and trial vector $t^{g+1}_{n,i}$ in the selection process. For the following generation, those that provide the lowest function value, or the best fitness function, are chosen. These operations are repeated until the predetermined value of generation is reached. The outcome or the best objective function solution in the present population is written as $Y_{best,G}$.

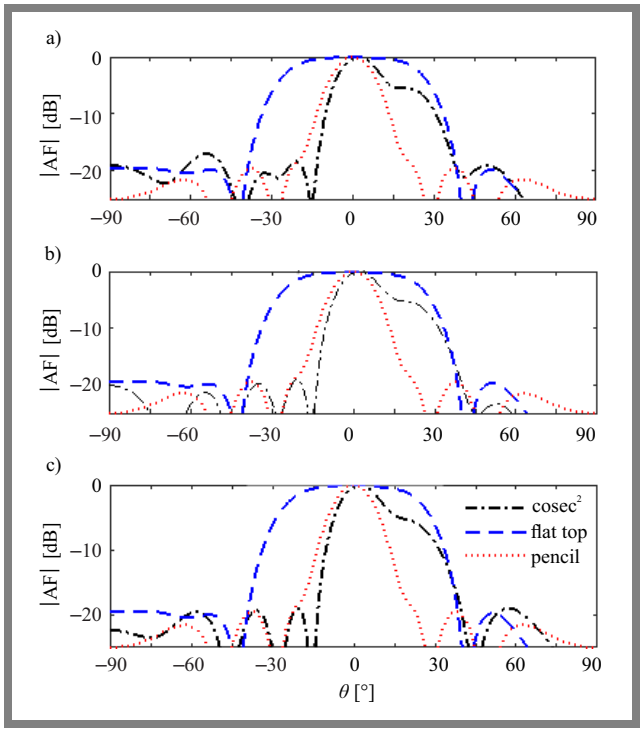

Fig. 3. DE utilized to produce various beam patterns for: a) $\varphi = 0°$, b) $\varphi = 5°$, and c) $\varphi = 10°$planes.

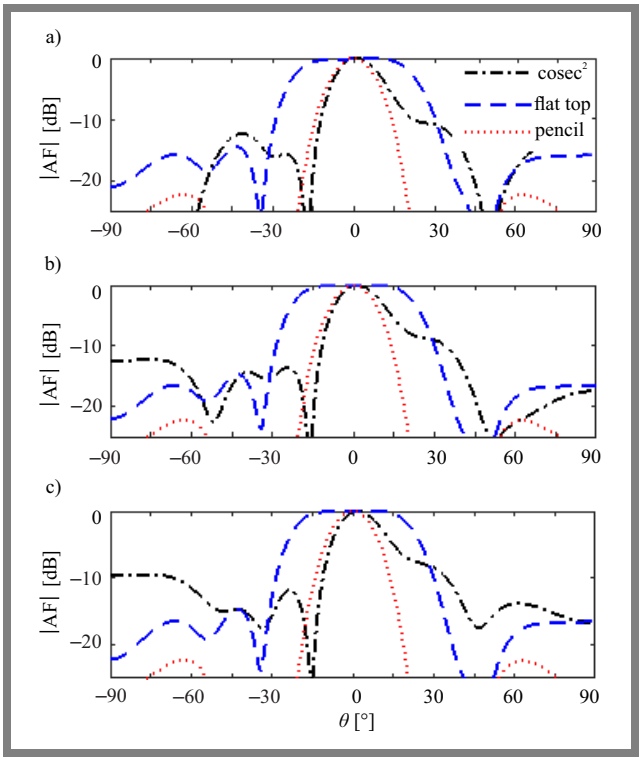

Fig. 4. FA utilized to produce various beam patterns for: : a) $\varphi = 0°$, b) $\varphi = 5°$, and c) $\varphi = 10°$planes.

The population size for such an optimization model is set to 50, the scaling factor (F) is set at 0.8, and indeed the DE's configured crossover rate (CR) is 0.2. This non-linear challenge is solved using the $DE/best/1/bin$ technique, with iterations up to 3000 [20]–[26].

3.2. Parametric Setup of Genetic Algorithm and Firefly Algorithm

The genetic algorithm (GA) [4], [30]–[34] is a technique that is capable of solving not only particular problems. It also allows to study in a direction where practice of interconnection with natural-inspired modification and significance of these in computation. With the purpose of discovering true solutions of fitness functions, GA is a helpful searching methodology commonly applied in computing. It is an evolutionary algorithm which is stimulated by evolutionary biology. The most straightforward GA has three types of operators, including selection, crossover, and mutation. Usually, this evolution method involves a population that is generated randomly using specific individuals. Here, each possible solution is known as an individual and the group of all individuals is called the population. For the GA algorithm, a significantly higher proportion of individuals or chromosomes makes up a set of artificially adapted structures at position t. The initial batch of individuals is generated at random, so each individual is subsequently built using a selection process and a collection of operators. Step 1 creates the initial iteration, is followed by step 2 creating the next iteration, and so on. This means that GA utilities sequence t to start generating a correct number of chromosomes for another iterative pro-

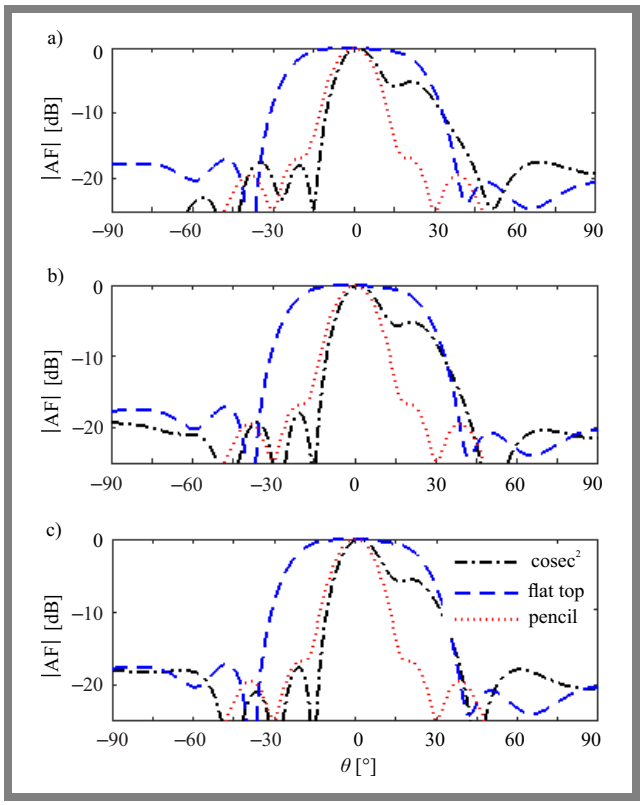

Fig. 5. GA utilized to produce various beam patterns for: a) $\varphi = 0^\circ$, b) $\varphi = 5^\circ$, and c) $\varphi = 10^\circ$planes.

cess at time $t + 1$. The algorithm performs between 1 and T repetitions, where T is a fixed variable or the stage where the most powerful individual is found or another terminating requirement is fulfilled.

The swarm-based firefly algorithm (FA) [14], [27]–[29] is based on the assumption that the majority of fireflies of nearly two thousand species produce short and rhythmic flashes. Although these are unisexual insects, regardless of their sex, every firefly is attracting too many other fireflies. The pattern by which both males and females attract each other is created using rhythmic flashes. The rate of the flashing and the duration of each blink are monitored. Brighter fireflies are attracted to those fireflies with a lower level of brightness. The flashing light is produced by bioluminescence, and the precise functions of such a communication system are indeed up for discussion. However, these flashes serve two main purposes: to draw in potential prey and to draw in mates (communication). Flashing can also serve as a warning mechanism for safety.

The two-point crossover strategies are chosen with a population size of 50 in GA. The odds for both crossover and mutation are set at 0.08 and 0.01, respectively. For this suggested scenario, the roulette wheel method is considered throughout the selection procedure, and just a termination or ending condition of a limit of 3000 iterations is selected as the method applied. Additional GA variable configurations are chosen from the list provided in [4], [30]–[34]. In FA [14], [27]–[29], 50 fireflies were taken, with $\gamma = 0.25$, $\beta_0 = 0.20$, $\alpha = 1$. The search space dimension and 48 randomly selected fireflies are used as the original population, with the search space dimensions being taken into account (3000 at the most iterations).

A four circular rings of array consist of sixty isotropic components have been estimated. The number of components in each round is a factor of six, i.e. $6m$, where m denotes the count of the circles. The radius for the first, second, third and fourth ring is 0.4775λ, 0.9549λ, 1.4324λ and 1.9099λ, respectively. The population for DE and FA for each individual case is:

$$P = \big[I_{1,1}, I_{1,2}, \ldots, I_{1,6}, I_{2,1}, \ldots, I_{2,12}, I_{3,1}, \ldots, I_{3,18}, I_{41}, \ldots, I_{4,24}, \alpha 1_{1,1}, \alpha 1_{1,2}, \ldots, \alpha 1_{1,6}, \alpha 1_{2,1}, \ldots, \alpha 1_{2,12}, \alpha 1_{3,1}, \ldots, \alpha 1_{3,18}, \alpha 1_{4,1}, \ldots, \alpha 1_{4,24}, \alpha 2_{1,1}, \alpha 2_{1,2}, \ldots, \alpha 2_{1,6}, \alpha 2_{2,1}, \ldots, \alpha 2_{2,12}, \alpha 2_{3,1}, \ldots, \alpha 2_{3,18}, \alpha 2_{4,1}, \ldots, \alpha 2_{4,24}\big]. \quad (9)$$

The limits of the variable are:

$$0 \leqslant I_{mn} \leqslant 1; \quad -\pi \leqslant \alpha 1_{mn} \leqslant \pi; \quad -\pi \leqslant \alpha 2_{mn} \leqslant \pi\,, \quad (10)$$

where: $m = 1,\ 2,\ 3,\ 4$, for the first ring $n = 1,\ 2, \ldots, 6$, for the second ring $n = 1,\ 2, \ldots, 12$, for the third ring $n = 1,\ 2, \ldots, 18$, and for the fourth ring $n = 1, \ , 2, \ldots, 24$.

The number of elements in this case is set to 60 and corresponds to the length of the search process which expands to 180.

4. Results

An antenna with 60 equally spaced isotropic components has been proposed as a concentric circular ring array. Here, M is the number of concentric rings. 4 rings have been considered,

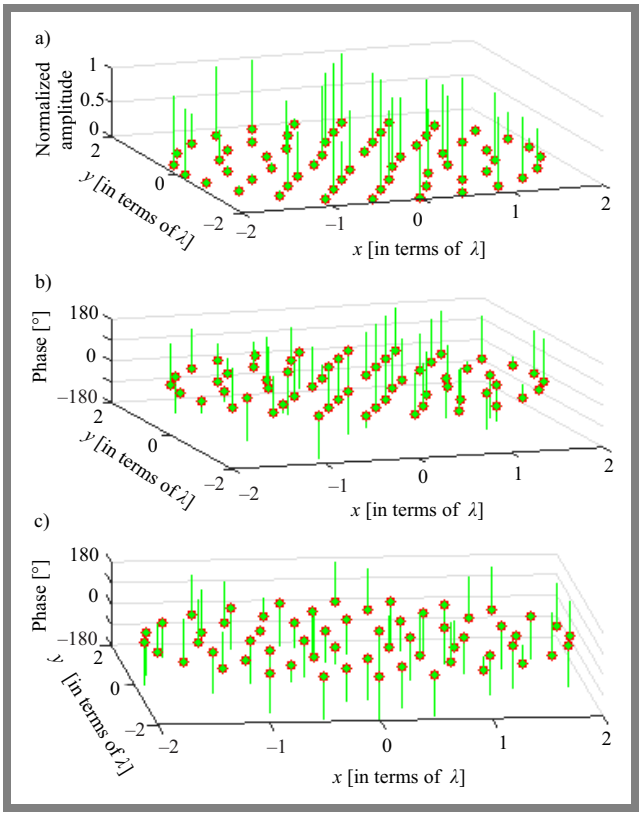

Fig. 6. Element-wise excitations using DE.

and each ring has N_m different components. This array has 6 isotropic elements in the first ring, 12 in the second, 18 in the third, and 24 in the fourth ring. The inter- element separation is taken into account and equals 0.5λ, as shown in Fig. 1. So, the ring radius becomes 0.4775λ for the first ring, 0.9549λ for the second ring, 1.4324λ for the third ring, and 1.9099λ for the fourth ring.

Tab. 1. Expected and achieved outcomes of the designed specifications.

φ cut	Beam type	Parameters [dB]		GA	FA	DE
0°	Flat top	$SLL_{\max}$	Expected	−20.00	−20.00	−20.00
			Achieved	−17.04	−14.51	−19.57
		Δ	Expected	0	0	0
			Achieved	20.85	21.95	21.76
	cosec^2	$SLL_{\max}$	Expected	−20.00	−20.00	−20.00
			Achieved	−16.82	−12.21	−17.05
		Δ	Expected	0	0	0
			Achieved	23.20	74.36	24.63
	Pencil	$SLL_{\max}$	Expected	−20.00	−20.00	−20.00
			Achieved	−16.77	−22.30	−18.08
5°	Flat top	$SLL_{\max}$	Expected	−20.00	−20.00	−20.00
			Achieved	−17.13	−14.76	−19.33
		Δ	Expected	0	0	0
			Achieved	21.93	18.16	22.79
	cosec^2	$SLL_{\max}$	Expected	−20.00	−20.00	−20.00
			Achieved	−17.69	−12.21	−18.17
		Δ	Expected	0	0	0
			Achieved	21.10	47.60	19.77
	Pencil	$SLL_{\max}$	Expected	−20.00	−20.00	−20.00
			Achieved	−16.77	−22.30	−18.08
10°	Flat top	$SLL_{\max}$	Expected	−20.00	−20.00	−20.00
			Achieved	−17.16	−14.71	−19.36
		Δ	Expected	0	0	0
			Achieved	21.91	18.11	22.77
	cosec^2	$SLL_{\max}$	Expected	−20.00	−20.00	−20.00
			Achieved	−17.15	−09.46	−18.05
		Δ	Expected	0	0	0
			Achieved	23.24	36.86	20.60
	Pencil	$SLL_{\max}$	Expected	−20.00	−20.00	−20.00
			Achieved	−16.77	−22.30	−18.08

Table 1 shows the design specifications for the multiple-beam patterns and the corresponding outcomes. It shows that the maximum side lobe level for the flat top beam pattern on 3 separate preset planes was achieved by applying DE and equaled −19.57 dB, −19.33 dB, and −9.36 dB, respectively, matching to its target value of −20.00 dB. The overall difference between the achieved and the intended values is calculated using the ripple Δ parameter within the angular region ($\theta = -15°$to +15°). The value of ripple Δ is 21.76 dB, 22.79 dB, and 22.77 dB for $\varphi = 0°$, $\varphi = 5°$and $\varphi = 10°$, respectively.

It has also been observed from Tab. 1 that using GA, the peak side lobe levels for the flat top radiation pattern in three separate preset planes ($\varphi = 0°$, $\varphi = 5°$, and $\varphi = 10°$) were achieved and correspond to the intended level of −20.00 dB at −17.4 dB, −17.13 dB, and −17.16 dB, with ripple Δ amounting to 20.85 dB, 21.93 dB, and 21.91 dB, respectively. The desired value of ripple Δ is 0 dB. The peak SLL as well as ripple Δ values (acquired and intended) obtained using FA are presented in Tab. 1. Maximum SLL is attained and equals −14.51 dB, −14.7 dB and −14.71 dB, with ripple Δ amounting to 21.95 dB, 18.76 dB, and 18.11 dB, respectively.

In contrast, the peak SLL for every pencil shaped beam pattern was measured to be −18.08 dB for DE, −16.77 dB for GA, and −22.30 dB for FA, when applied along the same predetermined azimuth planes.

From Tab. 1, it is additionally clear that the peak side lobe levels for the cosec^2 beam pattern along three separate preset planes were achieved employing the same DE method and equaled −17.05 dB, −18.17 dB, and −18.05 dB, respectively, in lieu of the desired value of −20.00 dB. Only within the angular range of ($\theta = 0°$o to 30°), the quantity ripple Δ is used to evaluate the overall discrepancy between the achieved and the intended quantities. For the azimuth angles of 0, 5, and 10°, the values of ripple Δ are 24.63 dB, 19.77 dB and 20.60 dB, respectively.

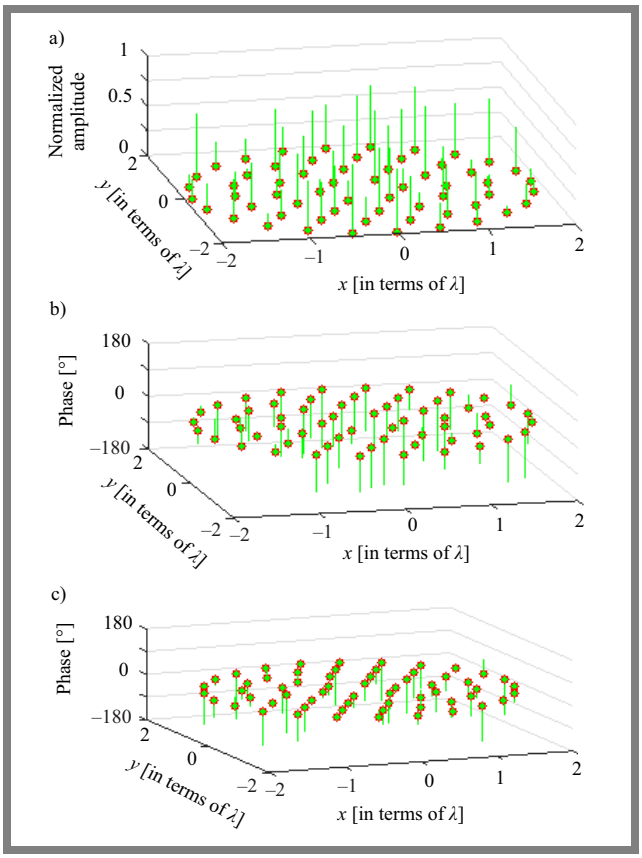

Fig. 7. Element-wise excitations using FA.

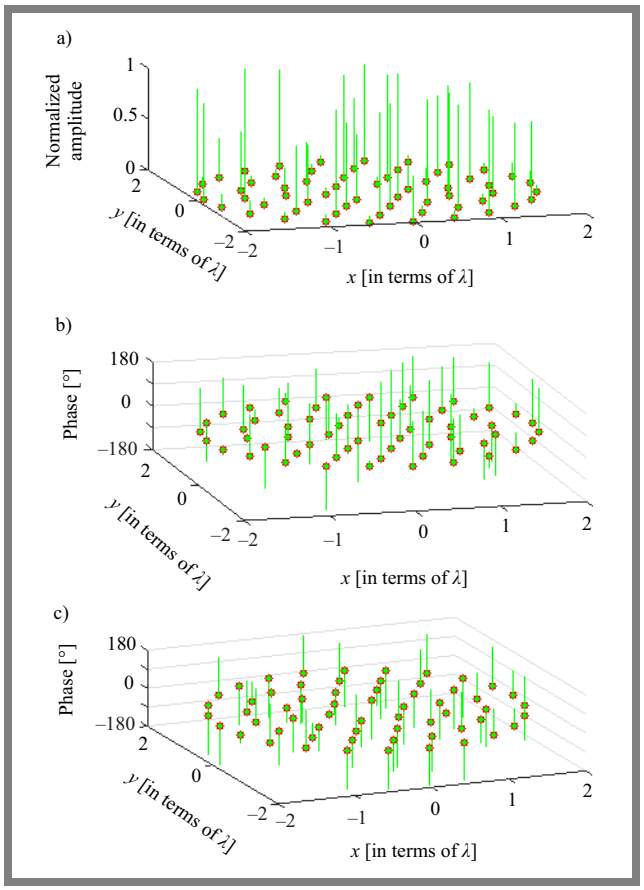

Fig. 8. Element-wise excitations using GA.

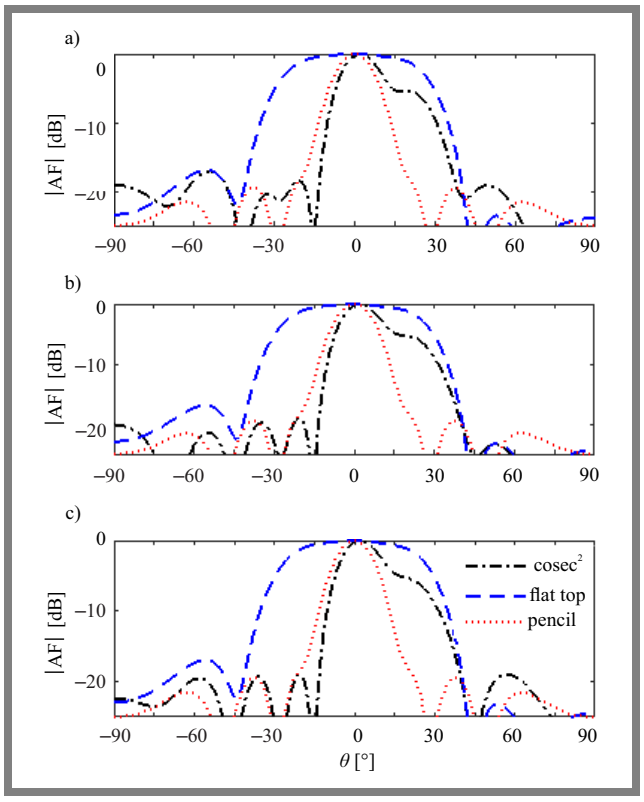

Fig. 9. Employing identical excitations acquired from DE, several shaped beam patterns have been achieved for three randomly selected planes: a) $\varphi = 2.5°$, b) $\varphi = 7.5°$, and c) $\varphi = 11.5°$.

Additionally, it is noted that using GA, peak side lobe levels obtained for the cosec^2 beam pattern in three distinct predetermined azimuth planes (0, 5, and 10°) are −16.82 dB, −17.69 dB, and −17.15 dB, respectively, compared to the desired level of −20.00 dB. Ripple Δ equals 23.20 dB, 21.10 dB, and 23.24, whereas the anticipated value is 0 dB. Similarly, Tab. 1 displays the expected and actual values of the FA's peak SLL and ripple Δ. Along with Δ of 74.36 dB, 47.60 dB, and 36.86 dB, the measured maximum SLL is −12.21 dB, −12.21 dB, and −09.46 dB.

The element-wise identical magnitudes of the array elements acquired employing DE, FA, and GA for creating multiple beam patterns are displayed in Figs. 6a, 7a, and 8a. These normalized magnitudes range from 0.625 to 1 and have 16 separate levels (2^4).

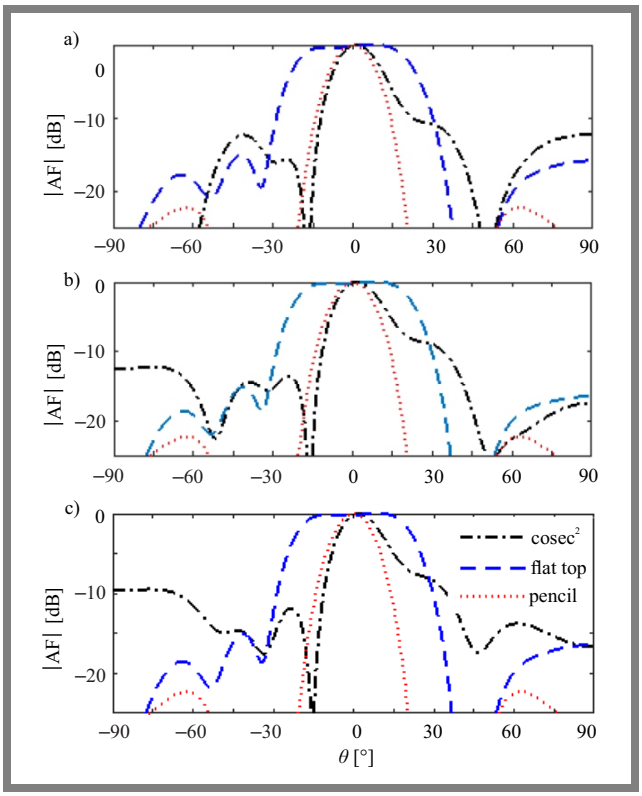

Fig. 10. Employing the identical excitations acquired from FA, several shaped beam patterns have been achieved for three randomly selected planes: a) $\varphi = 2.5°$, b) $\varphi = 7.5°$, and c) $\varphi = 11.5°$.

The DRR is lower, as the lowest value of normalized amplitudes is 0.625 and the highest value is 1. The proposed technique uses 4-bit amplitudes of the components in the array, which guarantees that the DRR remains lower than the 16-point restriction, which really is beneficial in terms of a dependable network feed arrangement. Separate excitations as well the decreased quantity of attenuators and phase shifters, will additionally lower the price and complexity of the mechanism.

Similarly, the phases having 2^5 i.e. 32 levels within –180° to +180°are incorporated. Such 5-bit discrete phases are shown in Figs. 6b-c, 7b-c, and 8b-c for DE, FA, and GA, respectively.

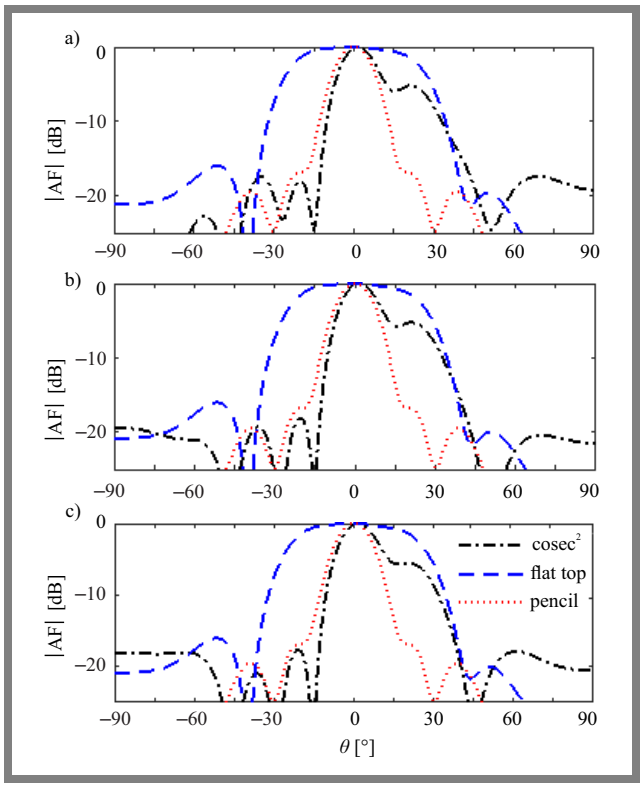

Fig. 11. Employing the identical excitations acquired from GA, several shaped beam patterns have been achieved for three randomly selected φ planes: a) $\varphi = 2.5^\circ$, b) $\varphi = 7.5^\circ$, and c) $\varphi = 11.5^\circ$.

Figure 6b shows the required phases applied for generating flat top beams, while Fig. 6c refers to the cosec^2 beam pattern with a common distribution of amplitudes. Figure 6a uses DE, whereas Figs. 7b and 8b show the required phases applied for generating flat top beams. Figures 7c and 8c relate to the cosec^2 beam pattern with a common distribution of amplitudes, while Figs. 7a and 8a are concerned with FA and GA, respectively.

In Figs. 9, 10, and 11, the same excitations result in somewhat different beam patterns in three randomly selected azimuth planes. The very first random azimuth angle in each figure is 2.5°(0°$<$ 2.5°$<$ 5°between the φ plane's boundaries), the second is 7.5°(inside the chosen φ plane of 5°and 10°), and the third is 11.5°($>$ 10°past the fixed azimuth plane), respectively.

The optimal excitations are produced using DE in both situations. Figure 3 depicts the multiple array pattern in predetermined azimuth planes and Fig. 9 depicts the patterns in randomly chosen azimuth planes. Additionally, Figs. 10 and 11 depict multiple array patterns in randomly selected azimuth planes, while Figs. 4 and 5 depict the patterns in predetermined φ planes. In both situations, the best excitations are produced using FA and GA in tandem.

The obtained flat top and cosec^2 beam patterns are following the desired beam patterns within the coverage range of –15°to +15°and 0°to 30°, respectively.

With all three EAs taken into consideration, the results of the design requirements are presented in Tab. 2 for random angles. Comparable design parameter values were found for φ planes that were chosen at random and those that were predetermined. Therefore, it is not necessary to take into account all azimuth planes for such an array synthesis technique. However, there are some preset azimuth planes that provide a span where the pattern retains the required feature. The converging curve for DE, FA, and GA algorithms is shown in Fig. 12. Such convergence curves make it obvious that DE is superior to FA and GA, since its fitness value is lower.

Tab. 2. Expected and achieved outcomes of the designed specifications.

φ cut	Beam type	Parameters [dB]	DE	FA	GA
2.5°	Flat top	$SLL_{\max}$	−16.91	−15.07	−15.99
		Δ	22.35	22.75	21.59
	consec^2	$SLL_{\max}$	−17.05	−12.21	−16.82
		Δ	24.63	74.36	23.20
	Pencil	$SLL_{\max}$	−18.08	−22.30	−16.77
7.5°	Flat top	$SLL_{\max}$	−16.90	−15.11	−15.99
		Δ	23.38	20.47	22.65
	consec^2	$SLL_{\max}$	−18.17	−12.21	−17.69
		Δ	19.77	47.60	21.10
	Pencil	$SLL_{\max}$	−18.08	−22.30	−16.77
11.5°	Flat top	$SLL_{\max}$	−16.93	−15.05	−16.02
		Δ	23.36	20.40	22.63
	consec^2	$SLL_{\max}$	−18.05	−09.46	−17.15
		Δ	20.60	36.86	23.24
	Pencil	$SLL_{\max}$	−18.08	−22.30	−16.77

Tab. 3. Comparison of DE, GA, and FA performance.

Algorithm	Best fitness (out of 15)	Worse	Mean	Standard deviation
DE	356.983	369.960	359.1682	3.1523
GA	390.444	408.513	397.5156	4.2589
FA	398.555	410.987	402.6547	4.4783

The accuracy of DE, FA, and GA is compared to show design-related difficulties (Tab. 3). The algorithm that turns out to be the best and most consistent in terms of this issue is DE, as it has a lower average fitness value than GA, PSO, and FA. As far as this kind of design requirements is concerned, Tab. 4 shows the results of the Wilcoxon rank sum test for

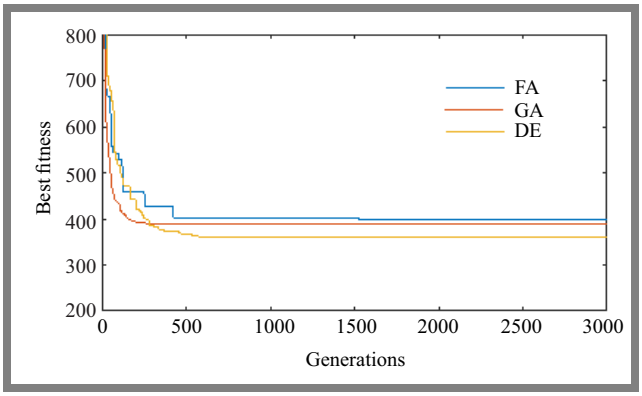

Fig. 12. Convergence curve for DE, GA, and FA.

Tab. 4. P-value for Wilcoxons two-sided rank sum test.

Contrasting pair	P-value
DE-GA	$3.3928 \cdot 10^{-6}$
DE-FA	$4.4938 \cdot 10^{-6}$

DE-FA and DE-GA pairings. The greatest support for the null hypothesis stating that the best final fitness value achieved by the best algorithm is statistically meaningful comes from any generated values that are lower than 0.05 (5% importance threshold).

5. Conclusions

In three separate azimuth planes, a multiple-beam concentric circular ring array antenna has been created employing three well-known evolutionary algorithms. Three separate beam patterns (flat top, cosec^2, and pencil beam) are created in three distinct azimuth planes. To achieve the necessary pattern characteristics, every evolutionary algorithm creates the best 4-bit discrete amplitudes as well as 5-bit discrete phases. The approach adopted demonstrates its capability to generate the very same beam pattern not only in the predetermined azimuth planes, but also across a span of azimuth planes, upon choosing and obtaining the identical pattern in random planes. By determining the ideal combination of array excitations using the DE, GA, plus the FA algorithm, such design requirements as peak side lobe level (peak SLL) and ripple Δ are decreased. By employing these digitized excitations, the dynamic range ratio is significantly decreased, thus requiring fewer attenuators and phase shifters in the circuit configuration.

References

[1] C.A. Balanis, *Antenna Theory: Analysis and Design*, 2nd edition. New York: Willy, 1997 (ISBN: 9780471592686).

[2] R.S. Elliott, *Antenna Theory and Design, Revised Edition*. Wiley – IEEE Press, 2002 (ISBN: 9780471449966).

[3] J.R. Mailloux, *Phased Array Antenna Handbook*, 2nd edition. Boston: Artech House, 2009 (ISBN: 9781580536899).

[4] Z. Michalewicz, *Genetic Algorithms + Data Structures*. Berlin, Heidelberg, New York: Springer, 1999 (ISBN: 9783540606765).

[5] X. Diaz, J.A. Rodriguez, F. Ares, and E. Moreno, "Design of phase- differentiated multiple pattern antenna arrays", *Microwave and Optical Technology Letters*, vol. 26, no. 1, pp. 52–53, 2000 (https://doi.org/10.1002/(SICI)1098-2760(20000705)26:1<52::AID-MOP16>3.0.CO;2-0).

[6] G. Buttazzoni and I.R. Vescovo, "Reconfigurable antenna arrays with phase-only control in the presence of near-field nulls", *Journal of Telecommunications and Information Technology*, no. 3, pp. 88–93, 2017 (https://doi.org/10.26636/jtit.2017.118817).

[7] J. Lei, G. Fu, L. Yang, and D.M. Fu, "Wide band linear printed antenna array with low sidelobe cosecant square-shaped beam pattern", *Progress in Electromagnetics Research C*, vol. 15, pp. 233–241, 2010 (https://doi.org/10.2528/PIERC10072506).

[8] O.M. Bucci, G. Mazzarella, and G. Panariello, "Reconfigurable arrays by phase-only control", *IEEE Transactions on Antennas and Propagation*, vol. 39, no. 7, pp. 919–925, 1991 (https://doi.org/10.1109/8.86910).

[9] G.K. Mahanti, A. Chakraborty, and S. Das, "Phase-only and amplitude-phase only synthesis of dual-beam pattern linear antenna arrays using floating-point genetic algorithms", *Progress in Electromagnetics Research*, vol. 68, pp. 247–259, 2007 (https://doi.org/10.2528/PIER06072301).

[10] M. Durr, A. Trastoy, and F. Ares, "Multiple-pattern linear antenna arrays with single prefixed amplitude distributions: modified Woodward-Lawson synthesis", *Electronics Letters*, vol. 36, no. 16, pp. 1345–1346, 2000 (https://doi.org/10.1049/el:20000980).

[11] S.K. Dubey and D. Mandal, "Digitally controlled steered dual beam pattern synthesis of a rectangular planar array antenna in a range of azimuth plane using evolutionary algorithms", *Progress in Electromagnetics Research C*, vol. 114, pp. 185–202, 2021 (https://doi.org/10.2528/PIERC21062303).

[12] A. Chakraborty, B. Das, and G. Sanyal, "Beam shaping using nonlinear phase distribution in a uniformly spaced array", *IEEE Transactions on Antennas and Propagation*, vol. 30, no. 5, pp. 1031–1034, 1982.

[13] W. Stutzman, "Synthesis of shaped-beam radiation patterns using the iterative sampling method", *IEEE Transactions on Antennas and Propagation*, vol. 19, no. 1, pp. 36–41, 1971 (https://doi.org/10.1109/TAP.1971.1139892).

[14] A. Chatterjee, G K. Mahanti, and A. Chatterjee, "Design of a fully digital controlled reconfigurable switched beam concentric ring array antenna using firefly and particle swarm optimization algorithm", *Progress in Electromagnetics Research B*, vol. 36, pp. 113–131, 2012 (https://doi.org/10.2528/PIERB11083005).

[15] A. Chatterjee, G.K. Mahanti, and R.P.S. Mahapatra, "Design of fully digital controlled reconfigurable dual-beam concentric ring array antenna using gravitational search algorithm", *Progress in Electromagnetics Research B*, vol. 18, pp. 59–72, 2011 (https://doi.org/10.2528/PIERC10101806).

[16] M.A. Mangoud and H.M. Elragal, "Antenna array pattern synthesis and wide null control using enhanced particle swarm optimization", *Progress in Electromagnetics Research B*, vol. 17, pp. 1–14, 2009 (https://doi.org/10.2528/PIERB09070205).

[17] D. Mandal, J. Tewary, K.S. Kola, and V.P. Roy, "Synthesis of dual beam pattern of planar array antenna in a range of azimuth plane using evolutionary algorithm", *Progress in Electromagnetics Research Letters*, vol. 62, pp. 65–70, 2016 (https://doi.org/10.2528/PIERL16060802).

[18] Y. Aslan, A. Roederer, and A. Yarovoy, "Concentric ring array synthesis for low side lobes: An overview and a tool for optimizing ring radii and angle of rotation", *IEEE Access*, vol. 9, pp. 120744–120754, 2021 (https://doi.org/10.1109/ACCESS.2021.3109171).

[19] Y. Jiang, S. Zhang, Q. Guo, and M. Li, "Synthesis of uniformly excited concentric ring arrays using the improved integer GA", *IEEE Antennas and Wireless Propagation Letters*, vol. 15, pp. 1124–1127, 2016 (https://doi.org/10.1109/LAWP.2015.2496173).

[20] R. Storn and K. Price, "Differential evolution: a simple and efficient heuristic for global optimization over continuous spaces", *Journal of Global Optimization*, vol. 11, no. 4, pp. 341–359, 1997 (https://doi.org/10.1023/A:1008202821328).

[21] K.V. Price, R. Storn, and J.A. Lampinen, *Differential Evolution – A Practical Approach to Global Optimization*. New York: Springer, 2005 (ISBN: 9783540209508).

[22] S. Das, A. Abraham, U.K. Chakraborty, and A. Konar, "Differential evolution using a neighborhood-based mutation operator", *IEEE Transactions on Evolutionary Computation*, vol. 13, no. 3, pp. 526–553, 2009 (https://doi.org/10.1109/TEVC.2008.2009457).

[23] J. Guo and J. Li, "Pattern synthesis of conformal array antenna in the presence of platform using differential evolution algorithm", *IEEE Transactions on Antennas and Propagation*, vol. 57, no. 9, pp. 2615–2621, 2009 (https://doi.org/10.1109/TAP.2009.2027046).

[24] Q. Xiaomei, H. Zhehuang, and C. Yidong, "An improved differential evolution algorithm based on adaptive parameter", *Journal of Control Science and Engin.*, vol. 2013, 2013 (https://doi.org/10.1155/2013/462706).

[25] S. Yang, Y.B. Gan, and A. Qing, "Sideband suppression in time-modulated linear arrays by the differential evolution algorithm", *IEEE Transactions on Antennas and Propagations Letters*, vol. 1, no. 1, pp.173–175, 2002 (https://doi.org/10.1109/LAWP.2002.807789).

[26] A. Massa, M. Pastorino, and A. Randazzo, "Optimization of the directivity of a monopulse antenna with a subarray weighting by a hybrid differential evolution method", *IEEE Transactions on Antennas and Propagations Letters*, vol. 5, no. 1, pp. 155–158, 2006 (https://doi.org/10.1109/LAWP.2006.872435).

[27] X.S. Yang, "Firefly algorithms for multimodal optimization", in *Stochastic Algorithms: Foundations and Applications*. *LNCS*, vol. 5792, pp. 169–178, 2009 (https://doi.org/10.1007/978-3-642-04944-6_14).

[28] S. Łukasik and S. Żak, "Firefly algorithm for continuous constrained optimization tasks", in *Computational Collective Intelligence*. *Semantic Web, Social Networks and Multi agent Systems*. *LNCS*, vol. 5796, pp. 97–106, 2009 (https://doi.org/10.1007/978-3-642-04441-0_8).

[29] X.S. Yang, *Engineering Optimization: An Introduction with Metaheuristic Applications*. Wiley, 2010 (ISBN: 9780470582466).

[30] R.L. Haupt, "Introduction to genetic algorithms for electromagnetics", *IEEE Antennas and Propagation Magazine*, vol. 37, no. 2, pp. 7–15, 1995 (https://doi.org/10.1109/74.382334).

[31] K.F. Man, K.S. Tang, and S. Kwong, "Genetic algorithms: Concepts and applications", *IEEE Transactions on Industrial Electronics*, vol. 43, no. 5, pp. 519–534, 1996 (https://doi.org/10.1109/41.538609).

[32] J.M. Johnson and Y. Rahmat-Samii, "Genetic algorithms in engineering electromagnetics", *IEEE Antennas and Propagation Magazine*, vol. 39, no. 4, pp. 7–21, 1997 (https://doi.org/10.1109/74.632992).

[33] D. Marcano, and F. Duran, "Synthesis of antenna arrays using genetic algorithm", *IEEE Antennas and Propagation Magazine*, vol. 42, no. 3, pp. 12–20, 2000 (https://doi.org/10.1109/74.848944).

[34] M.A. Panduro, A.L. Mendez, R. Dominguez, and G. Romero, "Design of non-uniform circular antenna arrays for side lobe reduction using the method of genetic algorithms", *International Journal of Electronics and Communications*, vol. 60, no. 10, 713–717, 2006 (https://doi.org/10.1016/j.aeue.2006.03.006).

Sanjay Kumar Dubey
Associate Professor
https://orcid.org/0000-0001-6066-6590
K. K. University, Bihar, India

Debasis Mandal
Professor and Registrar
https://orcid.org/0000-0003-2170-3576
E-mail: dr.debasis1984@gmail.com
Department of Electronics and Communication Engineering,
Ramchandra Chandravansi University,
Bishrampur, Palamu, Jharkhand, India